The Company of **Biologists**

RESEARCH ARTICLE

Minimizing the cost of locomotion with inclined trunk predicts crouched leg kinematics of small birds at realistic levels of elastic recoil

Christian Rode[1],[*],[‡], Yefta Sutedja[1],[*], Brandon M. Kilbourne[2],[3], Reinhard Blickhan[1] and Emanuel Andrada[1],[2]

ABSTRACT

Small birds move with pronograde trunk orientation and crouched legs. Although the pronograde trunk has been suggested to be beneficial for grounded running, the cause(s) of the specific leg kinematics are unknown. Here we show that three charadriiform bird species (northern lapwing, oystercatcher, and avocet; great examples of closely related species that differ remarkably in their hind limb design) move their leg segments during stance in a way that minimizes the cost of locomotion. We imposed measured trunk motions and ground reaction forces on a kinematic model of the birds. The model was used to search for leg configurations that minimize leg work that accounts for two factors: elastic recoil in the intertarsal joint, and cheaper negative muscle work relative to positive muscle work. A physiological level of elasticity (∼0.6) yielded segment motions that match the experimental data best, with a root mean square of angular deviations of ∼2.1 deg. This finding suggests that the exploitation of elastic recoil shapes the crouched leg kinematics of small birds under the constraint of pronograde trunk motion. Considering that an upright trunk and more extended legs likely decrease the cost of locomotion, our results imply that the cost of locomotion is a secondary movement criterion for small birds. Scaling arguments suggest that our approach may be utilized to provide new insights into the motion of extinct species such as dinosaurs.

KEY WORDS: Avian locomotion, Charadriiform birds, Kinetics, Optimization, Leg work

INTRODUCTION

The locomotion of small birds is characterized by a crouched posture. This posture could, for example, relate to the bird's ability to deal with rough terrain (Blum et al., 2011) or to power requirements (Usherwood, 2013). Although these suggestions can account for the general use of crouched posture, they cannot explain the complex motion of the segments during the stance phase. Theoretically, animals can use an infinite number of limb segment kinematics during locomotion. Nevertheless, they confine themselves to certain motion patterns (e.g. Fischer et al., 2002; Stoessel and Fischer, 2012) that are typically unique and not transferrable between species with different leg geometries (Gatesy and Pollard, 2011). This suggests the existence of criteria such as

[1]Department of Motion Science, Institute of Sport Science, Friedrich-Schiller-University Jena, Jena 07749, Germany. [2]Institute of Systematic Zoology and Evolutionary Biology with Phyletic Museum, Friedrich-Schiller-University Jena, Jena 07743, Germany. [3]College for Life Sciences, Wissenschaftskolleg zu Berlin, Wallotstraße 19, Berlin 19143, Germany.
*These authors contributed equally to this work

‡Author for correspondence (christian.rode@uni-jena.de)

simplification of locomotor control (Ogihara et al., 2014) or economy of locomotion (Alexander, 1991; Günther et al., 2004) that govern the motion of the segments.

Economy is important in locomotion (Hoyt and Taylor, 1981; Rubenson et al., 2004; Nudds et al., 2011; Watson et al., 2011). Possible strategies related to economic locomotion with segmented legs include exploiting energy recovery, e.g. in muscles spanning the ankle (intertarsal joint in birds; Biewener, 1998; Roberts et al., 1997; Daley and Biewener, 2003; Higham et al., 2008), or minimizing the sum of joint torques (Alexander, 1991; Günther et al., 2004). Birds, however, have a pronograde trunk orientation and the ground reaction forces (GRF) do not point towards the pelvis but are aligned in front of the pelvis throughout stance instead (Andrada et al., 2013). This arrangement has been suggested to provide stability in locomotion (Andrada et al., 2014), but is associated with large hip torques. Assuming that stability is also important, the trunk motion and the global leg operation can be accepted as constraints when minimizing joint torques. This, however, would align the knee and intertarsal joint (ITJ) close to the GRF, leading to an extended ITJ configuration that is in contrast to that observed in small birds (Gatesy and Biewener, 1991). Hence, the minimization of joint torques seems not to govern the segment kinematics in small birds.

Here, we were curious whether small birds shape their sagittal plane segment movement for economic locomotion. To test this, we selected three closely related species that differ in leg length and leg segment proportions. We measured their joint kinematics and GRFs during locomotion. Then, imposing the measured trunk movement and the GRF on a kinematic model of the bird, we searched for leg segment kinematics during stance that minimize the cost of locomotion. For this, we calculated leg work that accounted for the potential of energy recovery in the ITJ (Fig. 1C) and for metabolically cheaper negative muscle work relative to positive work (Woledge et al., 1985). Finally, we compared the segment kinematics corresponding to minimal leg work with experimental data.
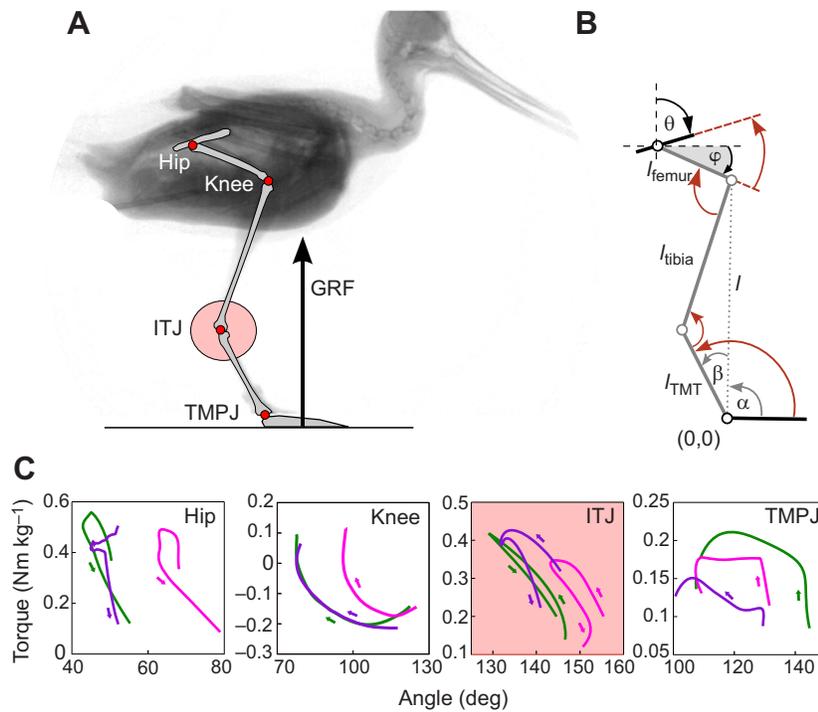
MATERIALS AND METHODS
Experiment and data acquisition

Four northern lapwings [*Vanellus vanellus* (Linnaeus 1758)], four Eurasian oystercatchers (*Haematopus ostralegus* Linnaeus 1758), and four pied avocets (*Recurvirostra avosetta* Linnaeus 1758), two male and two female for each species, approximately 1 year old, moved along a walking track at their preferred speeds. Kinematic data were recorded using high-speed biplanar X-ray videography (Neurostar, Siemens, Erlangen, Germany) at 1 kHz. GRFs and centre of pressure trajectories were obtained at 1 kHz from custom-built force plates (8×9 cm) with 6-degree-of-freedom force–torque sensors (ATI nano17, ATI Industrial Automation,

Fig. 1. Bird leg geometry and experimental torque-angle relationships from 10% to 80% stance.
(A) Kinematic and ground reaction force (GRF) data were obtained from latero-lateral X-ray projections of birds (here oystercatcher) traversing force plates. (B) Schematic with angle definitions. For given hip position relative to the tarsometatarsal-phalangeal joint (TMPJ), femur angle φ, and segment lengths, the positions of the knee and the intertarsal joint (ITJ) as well as the joint angles can be calculated (see Materials and methods, subsection 'Objective function of optimization'). (C) Only ITJ work loops of the lapwing (green), oystercatcher (magenta), and avocet (purple) show potential for elastic energy recovery.

Apex, NC, USA) integrated into the walking track. Kinematics and force data were recorded synchronously (post-trigger). The Committee for Animal Research of the State of Thuringia, Germany, approved the animal care and all experimental procedures (registry no. 02-47/10).

For our analysis, we neglected non-steady-state trials in which the difference in the horizontal velocity of the centre of mass between touchdown and lift-off was more than 10%. We then selected trials with touchdown speeds within 25% and 75% percentiles, resulting in 14 steps for lapwing, 17 steps for oystercatcher, and 12 steps for avocet (see Table 1). Leg landmarks [hip joint, knee joint, ITJ, and tarsometatarsal-phalangeal joint (TMPJ)] were tracked manually using SimiMotion software (SimiMotion Systems, Unterschleißheim, Germany). Data and scripts are freely available to download and use from http://dx.doi.org/10.6084/m9.figshare.1600900.

Objective function of optimization

We describe the cost of locomotion by leg work that accounts for two important factors: first, that muscles can recover energy stored in tendons (e.g. Roberts et al., 1997), which reduces metabolic cost; and second, that metabolic cost associated with negative muscle work is much lower than that of positive work (Woledge et al., 1985). Using the recorded trunk motion and GRF (Fig. 1) from 10% (where substantial GRF has developed) to 80% of the stance phase (where phalanges are still flat on the ground), leg kinematics of the model are varied until a minimum of the objective function, the leg work, is found.

Joint torque is calculated as the GRF magnitude times its perpendicular distance to the respective joint, ignoring effects of segment mass. Joint torque is positive for extension, that is, joint torque is positive for all joints except the knee in the example shown in Fig. 1A. Angles are defined accordingly (Fig. 1B, red). Joint work in a time interval is the mean joint torque multiplied by joint angular change within this interval (which corresponds to trapezoidal integration of the torque–angle relationship). To account for metabolically cheaper negative, eccentric muscle work, we scale negative joint work by a metabolic factor $M_{ecc} \in \{0, 0.1, \ldots, 0.5\}$, where 0 means no metabolic cost of negative work, and 0.5 means half the cost of negative work compared with positive work. The work W_i of the ith joint is calculated as the sum of positive work and absolute scaled negative work:

$$W_i(\varphi) = \sum_{j=2}^{n} \begin{cases} \tau_{ij}\Delta\delta_{ij}, & \tau_{ij}\Delta\delta_{ij} \geq 0 \\ M_{ecc}|\tau_{ij}\Delta\delta_{ij}|, & \tau_{ij}\Delta\delta_{ij} < 0 \end{cases}. \quad (1)$$

Here, φ is the vector of n femur angles spaced evenly across the selected fraction of the stance phase (counted with the index j), τ_{ij} is the mean value of the ith joint torque between the $(j-1)$th and the jth instant, and $\Delta\delta_{ij}$ is the angular change of the ith joint angle from the $(j-1)$th to the jth instant, i.e. $\Delta\delta_{ij}=\delta_{ij}-\delta_{ij-1}$. Joint angles δ_i are calculated for each time step using Eqns (2) to (6).

For given femur, tibiotarsus, and tarsometatarsus (TMT) lengths (l_{femur}, l_{tibia}, l_{TMT}) and chosen femur angle $\varphi(t)$, the locations of the knee and the ITJ relative to the TMPJ are given by:

$$\begin{pmatrix} x_{knee} \\ y_{knee} \end{pmatrix} = \begin{pmatrix} x_{hip} \\ y_{hip} \end{pmatrix} + l_{femur} \begin{pmatrix} \cos \varphi \\ -\sin \varphi \end{pmatrix} \quad (2)$$

and

$$\begin{pmatrix} x_{ITJ} \\ y_{ITJ} \end{pmatrix} = l_{TMT} \begin{pmatrix} \cos \delta_{TMPJ} \\ \sin \delta_{TMPJ} \end{pmatrix}, \quad (3)$$

where δ_{TMPJ} is the angle between the ground and the TMT, and (x_{hip}, y_{hip}) are the given coordinates of the hip joint relative to the TMPJ

Table 1. Number of animals, and the steps per animal

	Lapwing	Oystercatcher	Avocet
Number of animals	4	4	2
Steps per animal (right leg)	{3,1,1,1}	{3,1,6,1}	{3,2}
Steps per animal (left leg)	{3,1,3,1}	{1,1,3,1}	{3,4}

(Fig. 1B). Let $l=(x_{\text{knee}}^2+y_{\text{knee}}^2)^{0.5}$ be the virtual segment between the knee and the TMPJ and β the angle between this segment and the TMT. From the law of cosines it follows that:

$$\beta = \cos^{-1}\left(\frac{l_{\text{tibia}}^2 - l_{\text{TMT}}^2 - l^2}{-2ll_{\text{TMT}}}\right). \qquad (4)$$

The angle α between the ground and the virtual segment is given by:

$$\alpha = \cos^{-1}\left(\frac{x_{\text{knee}}}{l}\right). \qquad (5)$$

The joint angles follow from the leg geometry, the femur angle φ, and the prescribed trunk angle, θ (see Fig. 1B), as:

$$\begin{aligned}
\delta_{\text{TMTJ}} &= \alpha + \beta \\
\delta_{\text{ITJ}} &= \cos^{-1}\left(\frac{l^2 - l_{\text{TMT}}^2 - l_{\text{tibia}}^2}{-2l_{\text{TMT}}l_{\text{tibia}}}\right) \\
\delta_{\text{knee}} &= \delta_{\text{TMPJ}} + \delta_{\text{ITJ}} + \varphi - \pi \\
\delta_{\text{hip}} &= \frac{\pi}{2} - \theta + \varphi.
\end{aligned} \qquad (6)$$

In accordance with the potential for elastic recoil in the ITJ for all species (Fig. 1C; see Discussion), we simulated energy recovery by scaling the ITJ work obtained with Eqn 1 with $1-R_{\text{ITJ}}$ before summing the individual joint work to obtain the leg work, $W(\varphi)$. R_{ITJ} is a recovery factor that was varied in the optimizations ($R_{\text{ITJ}} \in \{0, 0.1, \ldots, 1\}$); 0 corresponds to no recovery, while 1 corresponds to full energy recovery, i.e. no cost of the work performed at the ITJ.

Optimization

We minimized the leg work for each species by optimizing the vector $\varphi(t)$ using the MATLAB (The MathWorks, Natick, MA, USA) algorithm GlobalSearch. GlobalSearch was developed to find the global minimum of a nonlinear multivariable objective function, in our case $W(\varphi)$. We set the lower bound for $\varphi(t)$ such that $l \leq (l_{\text{tibia}} + l_{\text{TMT}})$, and its upper bound as 60 deg. $\varphi(t)$ was a vector with $n=40$ data points throughout stance, and we set its initial values $\varphi_0(t)$ to 40 deg. We chose 5000 trial points, which resulted in approximately 250 different $\varphi_0(t)$ that converged in local solver runs for each optimization. GlobalSearch considered the minimum value of these to be the global minimum for one optimization.

To test our optimization results, we selected the R_{ITJ} and M_{ecc} that resulted in the lowest deviation between predicted and experimental segment angles for each species, and reran the optimization, but this time using five different initial conditions and the twofold number of trial points. The initial vectors of the femur angle $\varphi_0(t)$ were (1) those obtained from the data, (2) those corresponding to the lower bound and to the upper bound, respectively, and (3) constant angles throughout stance of 40 and 50 deg. The absolute deviation between these RMS values of segment angles and that of the standard optimization was 0.105±0.019, 0.052±0.021, and 0.002±0.001 deg for lapwing, oystercatcher, and avocet, respectively.

RESULTS

All three species with different leg geometries (Table 2, Fig. 2C) exhibited segment angle–time curves that were distinct from one another [root mean square (RMS) values of segment angle deviations comparing species data are 7.7 deg when comparing lapwings and oystercatchers, 5.2 deg when comparing lapwings and avocets, and 8.8 deg when comparing oystercatchers and avocets]. The mean femur angle of oystercatchers was approximately 10 deg

Table 2. Segment length (cm) comparison between species

Segment	Lapwing	Oystercatcher	Avocet
Femur	3.4	3.8	3.5
Tibiotarsus	6.2	8.2	10.2
TMT	4.1	4.2	8.1

steeper compared with that of lapwings and avocets. The tarsometatarsus started with a steeper angle in oystercatchers and reached the same angle as in lapwings at 80% stance. Avocets displayed generally a flatter tarsometatarsus angle throughout the stance phase.

Up to a certain threshold value of R_{ITJ} that decreased with increasing cost of negative work, the minimization of leg work resulted in a straight ITJ during stance for lapwings and oystercatchers (see plateaus in Fig. 2A and corresponding brown and orange stick figures in Fig. 2C), causing large deviations between predicted and experimental segment angle–time curves (Fig. 2B, brown and orange lines). Increasing the value of R_{ITJ} above this threshold led to a jump towards leg segment motion with bent ITJs, with moderate subsequent improvements towards a minimum in deviations (Fig. 2A,B, blue lines). Avocets, in contrast, did show bent ITJ configurations even when neglecting energy recovery, and showed moderate convergence to a minimum when increasing R_{ITJ} (Fig. 2, right column). Increasing R_{ITJ} above the value corresponding to minimal deviations (R_{ITJ} values of 0.5 for lapwings, 0.6 for oystercatchers, 0.6–0.8 for avocets) caused minimal leg work to decrease further (Fig. S1) but increased the segment deviations, with a clear minimum for lapwings and oystercatchers and a less clear minimum for avocets, albeit at very similar RMS values of segment angle deviations (lapwing 2.0 deg, oystercatcher 2.3 deg, avocet 2.1 deg). These values are low when compared with the deviations between the species (see above) and indicate a good approximation of the segment angle–time curves (Fig. S2).

Lapwings and oystercatchers showed rather clear minima of segment deviations between predicted and experimental data around M_{ecc} values of 0.2 and 0.1, respectively, while the minimum for avocets (indicated by the black cross within the blue range of the contour graph in Fig. 2C) was located in a shallow valley of small deviations that shifted smoothly from R_{ITJ} values of 0.6 to 0.8 when increasing the metabolic cost of negative work M_{ecc}.

DISCUSSION

Segment motions corresponding to minimized leg work best approximate the observed leg kinematics of the corresponding species (~2.1 deg RMS value of segment angle deviations) at 60% of energy recovery in the ITJ and at a realistic low metabolic cost of negative work (discussed below). This number agrees with values of elastic recoil reported for muscles spanning the ITJ in turkeys (Roberts et al., 1997). The exploitation of elastic recoil to reduce the cost of locomotion is reflected in the crouched segment kinematics of small birds.

Up to a certain threshold of energy recovery, segment configurations corresponding to minimized leg work showed a straight ITJ configuration during stance for lapwings and oystercatchers (Fig. 2). Only above this threshold is it more efficient for them to locomote with a bent ITJ. In avocets, even ignoring energy recovery led to leg configurations with a bent ITJ (Fig. 2C, turquoise stick figure). This might be related to their short femur length relative to total leg length compared with the other
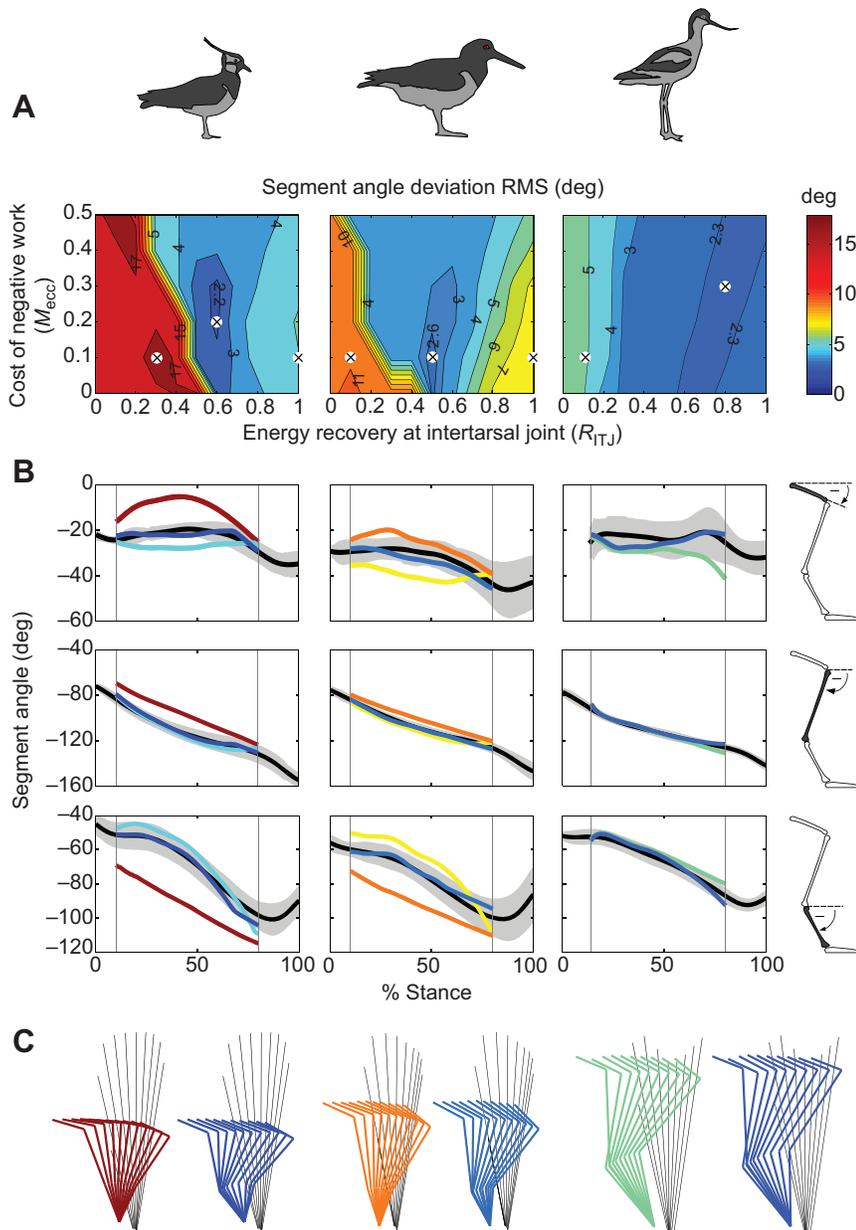
Fig. 2. Comparison of predicted and experimental segment angles. Columns, from left to right, correspond to lapwing, oystercatcher and avocet. (A) Contour graphs show the root mean square (RMS) deviations (in angular degrees) between predicted and experimental segment kinematics depending on the level of energy recovery at the intertarsal joint (R_{ITJ}) and on the metabolic cost of negative work (M_{ecc}). (B) Solid black lines in angle–% stance curves show average experimental data, the grey areas show experimental data standard deviation. The coloured segment angle–% stance curves correspond to combinations of R_{ITJ} and M_{ecc} indicated by crosses in contour graphs; colours reflect local RMS values of deviations. (C) Stick figures correspond to the coloured angle–% stance curves in B.

species, because for straight ITJ configurations, this would lead to large angular changes in the hip, resulting in large hip work.

We accounted for metabolically cheaper negative work by scaling the negative work with a metabolic factor, where 0 means no metabolic cost of negative work, and 0.5 means half the cost of negative work compared with positive work. The mean of the ratio of metabolic cost of stretch versus shortening at the same speeds is 0.33 (see Ma and Zahalak, 1991, their fig. 9), which is probably due to less ATP consumption by cross-bridges (Huxley, 1957) and titin–actin interactions (Rode et al., 2009). The effect of this low cost of stretch versus shortening is strengthened by the muscle's force–velocity relationship, which shows much larger forces during stretch than during shortening (Hill, 1938; Till et al., 2008). For example, if the muscle force corresponding to maximal positive muscle power is 0.4 of its maximum isometric force and a typical value of force during stretch is 1.30 of its maximum isometric force, then the metabolic cost associated with negative work would be 0.1 of the cost of the

same amount of positive work done at the same speed. Because of variations, for example, of contraction speeds, the metabolic cost factor may be expected to be in the range of 0.03 to 0.3 (a third to three times the estimate of 0.1). Hence, the minima between predicted and experimental deviations (Fig. 2A, crosses within blue ranges) seem very plausible, and we would certainly not expect the metabolic factor to exceed 0.5. Optimizations using unrealistically high metabolic factors (up to 1) led to more diffuse results with respect to minima in segment deviations and predicted levels of elasticity (Fig. S1). Hence, the effect of cheaper negative work should not be neglected.

Multi-articular muscles can modulate the joint-wise energy regime by transferring energy from joint to joint (Van Ingen Schenau, 1989) and thus hamper the identification of energy recovery in single-joint observations. In turkey and guinea fowl, elastic recoil was shown for the multi-articular gastrocnemius muscle–tendon complex spanning the ITJ (Roberts et al., 1997; Daley and Biewener, 2003; Higham et al., 2008). In another study,

Daley et al. (2007) reported spring-like behaviour of the ITJ in guinea fowl. The ITJ torque–angle relationship of the species investigated in the present study also approximated spring-like behaviour (Fig. 1C). This indicates that the length changes of multi-articular muscles such as the gastrocnemius could be dominated by the ITJ movement and that elastic recoil is reflected in the spring-like behaviour of this joint. This, together with the realistic predicted levels of energy recovery, suggests that the fundamental effect of energy recovery by muscle–tendon complexes in birds can be assessed using our approach. Follow-up studies considering the detailed anatomy of the leg and metabolic cost functions of muscles can refine the results presented here.

The leg movement of birds is not restricted to the sagittal plane (Stoessel and Fischer, 2012). Consequently, the sum of all segment angles of our model using constant segment lengths does not necessarily equal that of the measured angles at each instant (Fig. 2). Nevertheless, the predicted angles are in surprisingly good agreement with the measured angles. The examination of our findings with more sophisticated models approximating the three-dimensional motion of leg segments about natural joints with multiple degrees of freedom could lead to more confidence regarding the interpretation of our results.

In the present study, we used the trunk motion and the GRF as constraints while minimizing leg work during stance. An altered trunk posture, for example, an erect trunk, would lead to a decrease in leg work (Blickhan et al., 2015). Also, more extended leg configurations minimizing muscle forces can reduce leg work (Alexander, 1991). Still, birds use inclined trunk orientation inherited from their non-avian dinosaur ancestors, as well as crouched leg posture. This implies that other movement criteria may be more important than leg work minimization in bird locomotion. Constraints of muscle performance (Usherwood, 2013) have been suggested to determine the choice of leg posture in species of different size. Also, crouched legs in smaller species provide the ability to cope with relatively large changes in ground level (Blum et al., 2011). However, this would not straightforwardly explain the heavy trunk pitch in birds. This trunk posture seems to facilitate stable locomotion in birds (Andrada et al., 2014). Because our constrained minimization of leg work approximated the experimental segment kinematics, we suggest that minimizing the cost of locomotion is important, but comes second to other mentioned movement criteria for the investigated bird species; stability might be a candidate that could explain the pronograde trunk orientation.

Our study suggests that relatively small charadriiform bird species shape their segment kinematics to minimize leg work while exploiting elastic recovery during locomotion. We presume that these results can be extrapolated to larger species. For dynamically similar gaits, the mass-specific work per step is proportional to step length (Usherwood, 2013). Hence, minimization of leg work by shaping segment kinematics can be expected for larger species if they travel longer distances than their smaller counterparts and, vice versa, becomes less important for smaller species. Future studies on smaller and larger bird species such as quails and emus or ostriches, respectively, may confirm this. If our approach can be generalized, it might even be applied to gain insight into the motion of extinct taxa such as dinosaurs.

In conclusion, the exploitation of elastic recoil shapes the stance phase's segment movement in small birds; however, reducing the cost of locomotion is only a secondary movement criterion. Our approach may be exploited to predict the segment motions of extinct species.

Author contributions
R.B. and E.A. conceived the study. B.M.K. and E.A. conducted the experiments. C.R., Y.S. and E.A. analysed the experimental data. C.R. and Y.S. ran the optimizations. C.R. and Y.S. drafted the manuscript. All authors contributed to the interpretation of the results and revised the manuscript.

References
Alexander, R. M. (1991). Energy-saving mechanisms in walking and running. *J. Exp. Biol.* **160**, 55-69.

Andrada, E., Nyakatura, J. A., Bergmann, F. and Blickhan, R. (2013). Adjustments of global and local hindlimb properties during terrestrial locomotion of the common quail (*Coturnix coturnix*). *J. Exp. Biol.* **216**, 3906-3916.

Andrada, E., Rode, C., Sutedja, Y., Nyakatura, J. A. and Blickhan, R. (2014). Trunk orientation causes asymmetries in leg function in small bird terrestrial locomotion. *Proc. R. Soc. B Biol. Sci.* **281**, 20141405.

Biewener, A. A. (1998). Muscle function *in vivo*: a comparison of muscles used for elastic energy savings *versus* muscles used to generate mechanical power. *Am. Zool.* **38**, 703-717.

Blickhan, R., Andrada, E., Müller, R., Rode, C. and Ogihara, N. (2015). Positioning the hip with respect to the COM: consequences for leg operation. *J. Theor. Biol.* **382**, 187-197.

Blum, Y., Birn-Jeffery, A., Daley, M. A. and Seyfarth, A. (2011). Does a crouched leg posture enhance running stability and robustness? *J. Theor. Biol.* **281**, 97-106.

Daley, M. A. and Biewener, A. A. (2003). Muscle force-length dynamics during level *versus* incline locomotion: a comparison of *in vivo* performance of two guinea fowl ankle extensors. *J. Exp. Biol.* **206**, 2941-2958.

Daley, M. A., Felix, G. and Biewener, A. A. (2007). Running stability is enhanced by a proximo-distal gradient in joint neuromechanical control. *J. Exp. Biol.* **210**, 383-394.

Fischer, M. S., Schilling, N., Schmidt, M., Haarhaus, D. and Witte, H. (2002). Basic limb kinematics of small therian mammals. *J. Exp. Biol.* **205**, 1315-1338.

Gatesy, S. M. and Biewener, A. A. (1991). Bipedal locomotion: effects of speed, size and limb posture in birds and humans. *J. Zool.* **224**, 127-147.

Gatesy, S. M. and Pollard, N. S. (2011). Apples, oranges, and angles: comparative kinematic analysis of disparate limbs. *J. Theor. Biol.* **282**, 7-13.

Günther, M., Keppler, V., Seyfarth, A. and Blickhan, R. (2004). Human leg design: optimal axial alignment under constraints. *J. Math. Biol.* **48**, 623-646.

Higham, T. E., Biewener, A. A. and Wakeling, J. M. (2008). Functional diversification within and between muscle synergists during locomotion. *Biol. Lett.* **4**, 41-44.

Hill, A. V. (1938). The heat of shortening and the dynamic constants of muscle. *Proc. R. Soc. B Biol. Sci.* **126**, 136-195.

Hoyt, D. F. and Taylor, C. R. (1981). Gait and the energetics of locomotion in horses. *Nature* **292**, 239-240.

Huxley, A. F. (1957). Muscle structure and theories of contraction. *Prog. Biophys. Chem.* **7**, 255-318.

Ma, S. and Zahalak, G. I. (1991). A distribution-moment model of energetics in skeletal muscle. *J. Biomech.* **24**, 21-35.

Nudds, R. L., Folkow, L. P., Lees, J. J., Tickle, P. G., Stokkan, K.-A. and Codd, J. R. (2011). Evidence for energy savings from aerial running in the Svalbard rock ptarmigan (*Lagopus muta hyperborea*). *Proc. R. Soc. B Biol. Sci.* **278**, 2654-2661.

Ogihara, N., Oku, T., Andrada, E., Blickhan, R., Nyakatura, J. N. and Fischer, M. S. (2014). Planar covariation of limb elevation angles during bipedal locomotion in common quails (*Coturnix coturnix*). *J. Exp. Biol.* **217**, 3968-3973.

Roberts, T. J., Marsh, R. L., Weyand, P. G. and Taylor, C. R. (1997). Muscular force in running turkeys: the economy of minimizing work. *Science* **275**, 1113-1115.

Rode, C., Siebert, T. and Blickhan, R. (2009). Titin-induced force enhancement and force depression: a 'sticky-spring' mechanism in muscle contractions? *J. Theor. Biol.* **259**, 350-360.

Rubenson, J., Heliams, D. B., Lloyd, D. G. and Fournier, P. A. (2004). Gait selection in the ostrich: mechanical and metabolic characteristics of walking and running with and without an aerial phase. *Proc. R. Soc. B Biol. Sci.* **271**, 1091-1099.

Stoessel, A. and Fischer, M. S. (2012). Comparative intralimb coordination in avian bipedal locomotion. *J. Exp. Biol.* **215**, 4055-4069.

Till, O., Siebert, T., Rode, C. and Blickhan, R. (2008). Characterization of isovelocity extension of activated muscle: a Hill-type model for eccentric contractions and a method for parameter determination. *J. Theor. Biol.* **255**, 176-187.

Usherwood, J. R. (2013). Constraints on muscle performance provide a novel explanation for the scaling of posture in terrestrial animals. *Biol. Lett.* **9**, 20130414.

Van Ingen Schenau, G. J. (1989). From rotation to translation: constraints on multi-joint movements and the unique action of bi-articular muscles. *Hum. Mov. Sci.* **8**, 301-337.

Watson, R. R., Rubenson, J., Coder, L., Hoyt, D. F., Propert, M. W. G. and Marsh, R. L. (2011). Gait-specific energetics contributes to economical walking and running in emus and ostriches. *Proc. R. Soc. B Biol. Sci.* **278**, 2040-2046.

Woledge, R. C., Curtin, N. A. and Homsher, E. (1985). *Energetic Aspects of Muscle Contraction*. New York: Academic Press.